THE VELOCITY FIELD IN A VESSEL WITH ROTATING CYLINDER EQUIPPED WITH RADIAL BLADES*

I. Fořt, M. Ludvík and J. Čížp

Department of Chemical Engineering,
Institute of Chemical Technology 166 28 Prague 6

Received February 2nd, 1973

The Reynolds equations are solved for the turbulent flow of a fluid in an equipment formed by two coaxial cylinders the inner of which (rotating) is equipped with radial blades. The method of solution is that applied by Kármán and Prandtl to the flow in a circular pipe. The result of the solution is the radial profile of the dimensionless tangential component of the mean velocity in the form of a universal velocity profile in the given system. The analytical solution was compared with the experimentally found velocity field in the space between the outer edge of the rotating blades and the outer fixed cylinder. The results have confirmed the justification of the general analytical solution of the flow in the given system and were further used to calculate the parameter of the universal velocity profile for the system considered.

An equipment with a smooth rotating cylinder designed for dispersion of two liquids has been described by Clay[1] and an analogous equipment for the study of transport phenomena in heterogeneous systems has been proposed by Gandhi and Estrin[2]. Existing studies deal with this set-up from the viewpoint of the laminar flow stability, momentum transfer and application to rheological measurements[3]. For turbulent flow studies appears interesting the paper of Ustimenko and coworkers[4] who distinguish two different cases depending on which of the cylinders is rotating. Under developed turbulence and rotation of the outer cylinder the radial profile of the dimensionless velocity $\bar{v}/\bar{v}_{max}$ is independent of the Reynolds number; in the opposite case certain relation between both quantities can be detected. The latter phenomenon the authors explain by stabilizing effect of the field of eccentric velocity acting on the liquid in the space between the cylinders. The value of the Reynolds number (defined in terms of the peripheral velocity of the rotating cylinder) is in both cases greater than $2 \cdot 10^4$. Under this type of flow the so called Taylor vortices[5,13] form within the system as helix lines around the inner cylinder. This phenomenon causes the radial component of the intensity of turbulence to exceed the tangential component by a factor of two. Mizushina and coworkers[6] measured the velocity field in a cylindrical vessel equipped with axially located impeller with perpendicular blades in dependence on its relative height. From their results processed with the aid of a numerical solution of the Reynolds equations of flow it follows that the flow in the space above and below the impeller, where it is not immediately affected by the motion of the blades, is predominantly a secondary tangential flow. The radial profile of the tangential component of the mean velocity in the space occupied by the blades is indirectly proportional to the radial distance but it includes also an additive term proportional to the radial component of the local mean velocity. The given profiles for relatively

* Part XXXVIII in the series Studies in Mixing; Part XXXVII: This Journal *38*, 3074 (1973).

wide blades agree well with the experimental data. Under the given conditions also the field of contours of constant intensity of turbulence, σ_Θ, is homogeneous as a whole without local compression of the lines.

From the review it is apparent that the source of the convective transport – the impeller, or the rotating cylinder – must be modified so as to give as much as homogeneous, yet intensive enough, field of the mean and fluctuation components of velocity. These facts were taken into consideration in design of the apparatus.

THEORETICAL

Consider a quasi-stationary turbulent flow of an incompressible fluid between two concentric cylinders as sketched in Fig. 1. The inner cylinder is equipped with radial blades and rotates. The frame of reference used for description is shown in Fig. 2. The following simplifying assumptions are introduced for the system considered: *1*) All viscous stresses are negligible in comparison with the turbulent ones. *2*) The system is axially symmetric. *3*) The effect of the bottom and the lid on the velocity field is negligible. *4*) The flow within the system takes place predominantly in the tangential direction; the radial and the axial components of the mean velocity may be

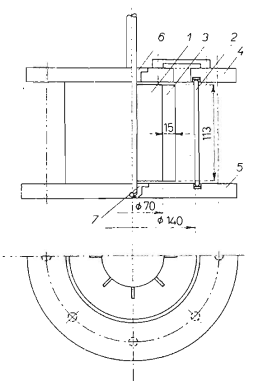

FIG. 1

A Sketch of Experimental Set-Up

1 Inner cylinder with radial blades, *2* outer smooth cylinder, *3* radial blades, *4* upper lid, *5* bottom lid, *6* packing, *7* lower bearing.

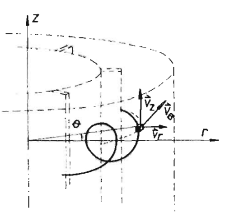

FIG. 2

The Frame of Reference in the Experimental Equipment

The origin of the z axis is on the lower edge of the rotating cylinder with radial blades.

neglected. *5*) The mean square fluctuation components $\overline{v_r'^2}$ and $\overline{v_\theta'^2}$ in a given position are equal. *6*) The tangential component of the mean velocity reaches its maximum $\bar{v}_{\theta\max}$, on the outer edge of the radial blades of the inner cylinder $(r = r)_1$.

From the Reynolds and the continuity equations for a quasi-stationary flow of an incompressible fluid in cylindrical coordinates[7] we get after simplification in accord with the above assumptions

$$\mathrm{d}\bar{p}/\mathrm{d}z = -\varrho_f \boldsymbol{g}\,, \quad r = \text{const.}\,, \tag{1}$$

$$\bar{v}_\theta^2/r = (1/\varrho_f)(\mathrm{d}\bar{p}/\mathrm{d}r)\,, \quad z = \text{const.}\,, \tag{2}$$

$$\mathrm{d}(\overline{v_r' v_\theta'})/\mathrm{d}r = -(2/r)(\overline{v_r' v_\theta'})\,. \tag{3}$$

By solving the set of Eqs (*1*) and (*2*) the distribution of the mean static pressure $\bar{p}$ in the system is obtained; from Eq. (*3*) then the radial profile of the component $\bar{v}_\theta$ of the mean velocity characterizing the flow within the system. On integrating Eq. (*3*) with the aid of the definition of the appropriate component of the turbulent stress tensor $\bar{\tau}^t_{\theta r}$ and the boundary condition $\bar{\tau}^t_{\theta r} = \tau_w$ for $r = R$ we get

$$\bar{\tau}^t_{\theta r} = \tau_w(R^2/r^2)\,. \tag{4}$$

In an analogous way as that leading to the universal logarithmic velocity profile in a pipe[8] we shall make use of the Kármán relation for the non-zero component of the turbulent stress[5] in which we substitute from Eq. (*4*) to get

$$\tau_w \frac{R^2}{r^2} = K^2 \varrho_f \frac{(\mathrm{d}\bar{v}_\theta/\mathrm{d}r)^2}{(\mathrm{d}^2\bar{v}_\theta/\mathrm{d}r^2)^2} \left|\frac{\mathrm{d}\bar{v}_\theta}{\mathrm{d}r}\right| \frac{\mathrm{d}\bar{v}_\theta}{\mathrm{d}r}\,. \tag{5}$$

Since $(\mathrm{d}\bar{v}_\theta/\mathrm{d}r) < 0$, we get from the Boussinesque relation[9] $\bar{\tau}^t_{\theta r} = \varepsilon(\mathrm{d}\bar{v}_\theta/\mathrm{d}r)$, that the viscous stress on the wall τ_w is always negative. Thus we may write

$$\frac{\mathrm{d}^2\bar{v}_\theta/\mathrm{d}r^2}{(\mathrm{d}\bar{v}_\theta/\mathrm{d}r)^2} = \frac{K}{v^*}\frac{r}{R}\,. \tag{6}$$

On integrating Eq. (*6*) with the boundary conditions expressing "no slip" of liquid on the wall of the fixed cylinder, *i.e.* $\mathrm{d}r/\mathrm{d}\bar{v}_\theta = 0$ for $r \to R$, and with the assumption *6*, $[\bar{v}_\theta(r_1) = \bar{v}_{\theta\max}]$, one obtains the result in dimensionless form as

$$\frac{\bar{v}_\theta(r)}{v^*} = -\frac{1}{K}\ln\frac{R+r}{R-r} + \frac{1}{K}\ln\frac{R+r_1}{R-r_1} + \frac{\bar{v}_{\theta\max}}{v^*}\,. \tag{7}$$

The quantity $\bar{v}_{\theta max}$ is eliminated in a manner similar to that used by Prandtl in case of a pipe[5]. Let us suppose that there exists a laminar sublayer Δr_1 thick on the wall of the outer cylinder. For its thickness Prandtl derived

$$\Delta r_1 = \beta(\nu/v^*)\,, \tag{8}$$

where β is a constant characterizing the flow within the laminar sublayer and its value has been determined experimentally[8] for similar flows to be equal $\beta = 11{\cdot}5$. For a relatively thin layer the radial profile of the velocity component in the sublayer $\bar{v}_\theta = \bar{v}_\theta(r)$ may be approximated by a linear profile assuming the Newton law of viscosity to hold in the given region and the tangential stress at $r_2 = R - \Delta r_1$ may be put equal to τ_w. Finally, we may write

$$\tau_w/\varrho_f = \nu[\mathrm{d}\bar{v}_\theta(r)/\mathrm{d}r]\,, \quad r \in \langle r_2; R\rangle\,. \tag{9}$$

On integrating the last equation in the limits r_2 and R and after some arrangement we get

$$\beta = \bar{v}_\theta(r_2)/v^*\,. \tag{10}$$

At r_2 we have also Eq. (7) in which we can substitute for the ratio $\bar{v}_\theta(r_2)/v^*$ from Eq. (10). The ratio $\bar{v}_{\theta max}/v^*$ may thus be expressed as

$$\frac{\bar{v}_{\theta max}}{v^*} = \beta + \frac{1}{K}\ln\frac{R + r_2}{R - r_2} - \frac{1}{K}\ln\frac{R + r_1}{R - r_1}\,. \tag{11}$$

The procedure leads to an expression for $\bar{v}_\theta(r)$:

$$v_\theta^+ \equiv \frac{\bar{v}_\theta(\varrho)}{v^*} = -\frac{2{\cdot}303}{K}\log\left(\frac{1 + \varrho}{1 - \varrho}\right) + \frac{2{\cdot}303}{K}\log\left(\frac{R + r_2}{R - r_2}\right) + \beta\,. \tag{12}$$

Quantity r_2 can be determined from

$$r_2 = R - \beta(\nu/v^*) \tag{13}$$

and K must be found from an experimental velocity profile $\bar{v}_\theta = \bar{v}_\theta(r)$. To determine v^* we start from the general equation for the pressure drop, which, in view of the assumption *3*, may be written in a form analogous to that for the flow between two parallel infinite plates

$$\Delta\bar{p}_{\theta z} = f\frac{2\pi R}{R - r_1}\frac{\bar{v}_{\theta max}^2}{4}\varrho_f\,. \tag{14}$$

From the balance of forces under quasi-stationary flow written in accord with assumption *3* we find for the tangential stress near the wall the following expression

$$\tau_w = [\Delta \bar{p}_{\theta z}(R - r_1)]/2\pi R \qquad (15)$$

and further, after some manipulation, an expression for the dynamic velocity

$$v^* = (f)^{1/2}\,(\bar{v}_{\theta \max}/2)\,. \qquad (16)$$

To calculate the friction factor f, Eq. (7) is written at $r = r_2$ with Δr_1, $\bar{v}_\theta(r_2)$ and v^* substituted by using Eqs (*8*), (*10*) and (*16*) respectively. Thus we obtain

$$f^{1/2} = +\,2K(\log\{[R(R - r_1)]/(R + r_1)\mathrm{Re}_m(f)^{1/2} - \beta(R - r_1)]\}/\beta(R - r_1)\} + \\ + K\beta)^{-1}\,. \qquad (17)$$

EXPERIMENTAL

Equipment. The equipment consists of two concentric cylinders, the outer is fixed and the inner rotates around its axis (see Fig. 1). The inner cylinder *1* is further equipped with six radial blades *3*. The arrangement and the dimensions are apparent from Fig. 1. The material used was brass and perspex glass (the outer cylinder 2 and both lids).

Measuring technique. The experimental technique was that of photographing the trajectories of tracer particles. The hot-wire anemometer technique was rejected for the present because of the difficulties associated with the disturbing effects of the probe on the flow in a relatively small experimental equipment. For tracer we took aluminum powder. The size of the powder particles was 10^{-4} m used at concentration 1·5 g/l. The suitability of the particles was verified by computing *a*) the slip velocity between the particles and the liquid (the velocity of the latter was taken 0·8 m/s) according to Pinkus[10], and *b*) the intensity of turbulence of the particles and the liquid according to Soo[11]. In the latter case the necessary value of the Lagrange macro-scale of turbulence was taken equal to 1 cm in accord with the measurements of Mujumdar and co-workers[12] under the conditions which were thought to be comparable with those in our experimental set-up. For the root mean square of the fluctuation velocity component we took 0·05 m/s as a mean value found by preliminary experiments. The obtained results have confirmed that the particles of the given size follow sufficiently accurately the convective flow and the turbulent pulsations (the slip velocity was virtually zero and the difference between the intensity of the turbulence of the particle and liquid was found smaller than 2%). To trace the paths of the aluminum particles we used a Pentaflex AK-16 motion picture camera (lens Meyer 2·8—100). The over-all arrangement of the recording set-up is apparent from Fig. 3. In order to achieve a sufficiently sharp and contrast image of the trajectories the whole apparatus was covered with black paper leaving only two slots. The first, 1·8 mm wide, in the bottom for the light, the other, 15 mm wide, in the lid for the camera. The projections of the trajectories were measured on enlarged negatives; the total enlargement being 8·53.

The time of exposure was taken so as to confine the length of the trajectories below the mesh size of the grid (1 mm) used to determine the local values of velocity components. The found depth of field for the given lens was 2·5 mm which is sufficient with regard to the magnitude of the quantities $|v'_\theta|$ and $|v'_r|$ which do not permit the particle to leave the photographed plane

during exposure. The velocities were averaged over a volume about 10^5 times smaller than the volume of the whole equipment which was though reasonable for preserving the local character of the measured quantities.

Accuracy. At the 30° angle and the frequency 20 s^{-1} the average deviation of the shutter speed was 1·3%. This value was found from measurement of the position of the pointer on the chronometer on 35 sequentially taken frames. The maximum deviation of the dermination of the position in the system was 0·2%. The fluctuation of the r.p.m. of the inner cylinder was 0·6% (the maximum deviation at the lowest r.p.m.). The maximum error of the dependent variables following from these deviations are: $\Delta v_\Theta = \pm 0{\cdot}018$ m/s and $\Delta v_r = \pm 0{\cdot}012$ m/s. If the error of the average of the above velocities is not to exceed 0·003 m/s, the number of measurements of the instantaneous local values must not drop below 40. The deviations of these averages then reach the following maximum values: $\Delta \bar{v}_\Theta = \pm 0{\cdot}0028$ m/s, $\Delta \bar{v}_r = \pm 0{\cdot}0017$m/s.

Experimental conditions. The velocity profiles and the profiles of the intensity of turbulence were measured in a plane perpedicular to the axis of the equipment passing through its center. Distilled water at 20 ± 0·5°C was used as liquid. The selected r.p.m. of the inner cylinder and the maximum (peripheral) tangential velocities were as follows: 147·0, 123·0, 100·4, 75·8 (min^{-1}) and 0·776, 0·650, 0·530, 0·400 (m s^{-1}).

RESULTS AND DISCUSSION

Radial Profiles of the Mean and Fluctuation Velocity Components

The tangential component of the mean velocity expressed as $\bar{V}_\Theta \equiv \bar{v}_\Theta / \bar{v}_{\Theta max}$ decreases uniformly (see Fig. 4) from the outer edge of the blades up to almost the wall of the fixed cylinder. A significant velocity gradient appears over a very short radial

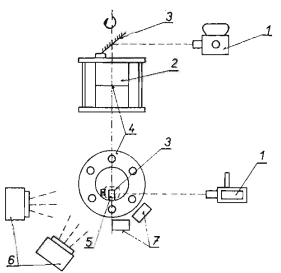

FIG. 3

A Sketch of Picture-Taking and Illumination Set-Up

1 Picture camera, *2* apparatus, *3* mirror, *4* slot, *5* slot in the lid, *6* 1 000 W lamps, *7* 800 W halogen floodlights.

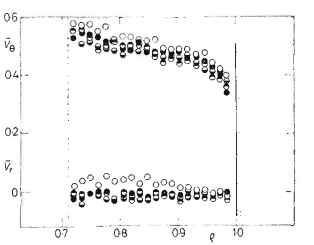

FIG. 4

Radial Profiles of the Mean Velocity Components

$\bar{v}_{\Theta max}$ (m s^{-1})	0·776	0·650	0·530	0·400
point	●	◒	◓	○

distance in the proximity of the rotating blades. This is apparently the source of the turbulence in the system contributing considerably to the different behaviour of the system in contrast to that consisting of two coaxial smooth cylinders. On the side of the fixed cylinder the course of the given component of the mean velocity is on the contrary in full agreement with the behaviour of the profile of the component of the mean velocity near the smooth wall: As a consequence of viscous forces the profile is steeper and one may expect the transient buffer layer[8] to appear between the laminar sublayer and the turbulent core of the flow.

The magnitude of the radial component of velocity expressed as $\overline{V}_r = \bar{v}_r/\bar{v}_{\vartheta max}$ remains small along the whole examined interval (see Fig. 4) and may be neglected in view of the accuracy of measurement since both positive and negative values appear randomly along the whole radius. Only certain values found at the lowest r.p.m. differ significantly from zero which is probably caused by the systematic error of measurement associated with the vortex formed between two neighbouring blades. At low r.p.m. this vortex gives rise to a significant secondary flow. The lower limit of the interval of r.p.m. should be thus regarded as being outside the validity limits of the presented theory. The Reynolds number still reaches $Re_m = 2{\cdot}2 \,.\, 10^4$; the proposed solution can be accepted as long as $Re_m > 2{\cdot}5 \,.\, 10^4$.

The experimentally found velocity profile $v_\vartheta^+ = v_\vartheta^+(\varrho^+)$ (Fig. 5) illustrates the adequacy of the correlation (*12*). The value of the parameter K, however, cannot be taken over from the results in a straight pipe. This value was found from the experiments (see Fig. 5) in an iterative manner, *i.e.* by succesive regression of the linear relation between v_ϑ^+ and ϱ^+ in which we had substituted for v^+ from Eqs (*16*) and

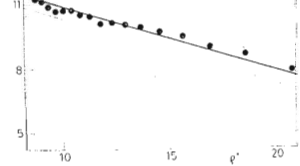

FIG. 5

Universal Logarithmic Velocity Profile between Two Coaxial Cylinders

The inner cylinder with the blades is rotating.

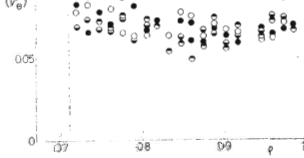

FIG. 6

Radial Profile of the Tangential Fluctuation Velocity Component

(*17*) and for K the value from the previous iteration step. The resulting K after the fourth iteration is $K = 1{\cdot}89$ while the first estimate from experiments in a straight pipe[8] was $K = 0{\cdot}4$. Fig. 5 shows the best straightline $v_\varrho^+ = v_\varrho^+(\varrho^+)$ for the value of K from the last iteration. The 95% confidence limits $v_\varrho^+ \pm 2\sigma_{v_\varrho^+}$ are shown there too. The values after the third and the fourth iteration did not differ by more than the accuracy of the calculation from the experiments. From the results it follows that the order of magnitude of K for our system and for a straight pipe of circular cross-section is almost the same but their identity could not be proven.

The radial profiles of the root mean square fluctuation components of the velocity display again certain important properties:

The dimensionless tangential component defined as $\overline{(V'^2_\Theta)}^{1/2} \equiv \overline{(v'^2_\Theta)}^{1/2}/(\bar{v}_{\Theta\max})$ remains almost constant over the whole investigated radius (see Fig. 6) excepting the immediate proximity of the inner fixed cylinder (discarding certain results carrying serious experimental error under the lowest r.p.m.).

The profile of the radial dimensionless component, defined as $\overline{(V'^2_r)}^{1/2} \equiv \overline{(v'^2_r)}^{1/2} : \bar{v}_{\Theta\max}$ becomes important starting from $\varrho = 0{\cdot}9$ (Fig. 7) up to the fixed cylinder where the decay of turbulence due to the presence of a solid surface at rest calls for a decrease of the given quantity. Extrapolating to $\varrho = 1$ one obtains practically a zero value.

The radial profile of the tangential component of turbulence defined as* $\sigma_\Theta \equiv \overline{(v'^2_\Theta)}^{1/2}/\bar{v}$ displays in the turbulent core (see Fig. 8) similar properties as the radial

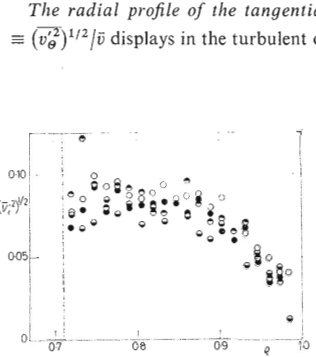

FIG. 7

Radial Profile of the Radial Fluctuation Velocity Component

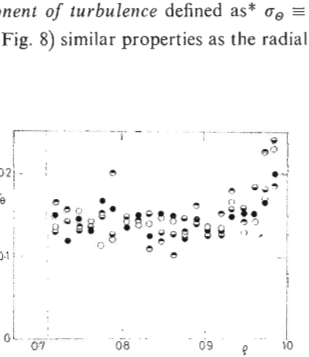

FIG. 8

Radial Profile of the Tangential Component of Intensity of Turbulence

* The absolute magnitude of the vector of local mean velocity $\bar{v}$ was computed as a vector product of $\bar{v}_\varrho$ and $\bar{v}_r$.

profile of $(\overline{V_\theta'^2})^{1/2}$; in region of the buffer layer, however, the value of σ_θ significantly increases and its eventual decrease in region of the laminar sublayer was not detected in the experiments since there was not enough traces of the aluminum powder in the proximity of the wall.

The radial component of the intensity of turbulence, defined as $\sigma_r \equiv (\overline{v'^2})^{1/2}/\bar{v}$, displays in contrast almost identical properties (see Fig. 9) along the radius. Somewhat different appears the region in the immediate proximity of the rotating blades where σ_r decreases with ϱ so that at $r = r_1$ the v'_θ component induced by the rotation of the blades prevails over v'_r.

It should be noted that the profiles near the top and the bottom lids will be affected by the presence of the solid surface at rest. However, the affected depth is small enough to occupy only an insignificant portion of the volume of the apparatus.

The Analysis of the Simplifying Assumptions of the Solution of the Reynolds Equation

On the basis of the experimental results one can now judge the adequacy of the assumptions made in the course of the solution.

The first of them could not be verified explicitly, however, the components of the intensity of turbulence, which in almost the whole system exceed 5%, confirm that the character of the flow in the whole equipment is turbulent. As an indirect proof of the validity of the assumption one can put forth *a*) the agreement of the proposed correlation between v_θ^+ and ϱ^+ which is typical for turbulent flow, and *b*) the mentioned minimum value of the Reynolds number Re_m in the system corresponding already to a fully developed turbulent flow. The assumption of negligible effect of the lids of the apparatus on the velocity field in the system, of course, does not hold in the proximity of the lids. The solution though was proposed for the bulk

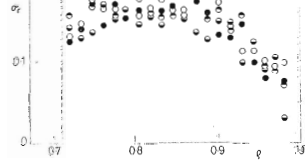

FIG. 9
Radial Profile of the Radial Component of Intensity of Turbulence

of the phase in the equipment which is acceptable in view of the preliminary experimental finding in the tangential plane showing the value of $\bar{v}_z$ negligible in the whole investigated interval. The fourth assumption for $\bar{v}_r$ has been confirmed (see Fig. 4). Negligible values of $\bar{v}_z$ over the investigated radius were also found in preliminary experiments and it may be expected that in view of the design of the apparatus a zero value of $\bar{v}_r$ in an incompressible fluid calls for zero value of $\bar{v}_z$ for continuity reasons.

The justification of the fifth assumption was proven in the whole examined interval excepting the proximity of the wall of the outer immobile cylinder. In this region the existence becomes important of the mentioned transient buffer layer and a more accurate solution would require introduction of another intermediate layer in addition to the laminar sublayer near the wall (in the sense of the semi-empirical solution for a pipe[5,8]). This approach, though providing a more accurate solution would complicate the solution excessively, especially at the succesive determination of the dispersion mechanism of the immiscible liquids in the system.

The sixth assumption implies that the number of revolution of the cylinder is so high that the liquid between the blades can be looked upon from the standpoint of its mean velocity as a rigid body rotating with the blades. Then indeed the maximum velocity in the system is that of the peripheral velocity of the edges of the blades. This consideration, of course, does not rule out the existence of pulsations of the velocity in the space between the blades, which then contribute to the increased level of intensity of turbulence in the batch.

A Comparison of the Velocity Profiles in a Straight Pipe and in the Proposed Apparatus

The course of the longitudinal component of the dimensionless mean velocity v_Θ^+ (or v_z^+ in the pipe) is the same[5,8] in principle for both systems compared, *i.e.* expressed as a logarithmic function of the dimensionless radial coordinate. A parameter in both cases is the maximum value of the dimensionless average velocity, or after arrangement, the value averaged over the whole cross section. In such a case even the auxiliary calculations (*e.g.* the calculation of the friction factor) do not differ. The course and the form of the radial profile is thus in both cases compared equivalent although in the case of cylinders of which one is fixed this relation is a monotonous function of spatial argument while in the pipe the given function has a maximum in the axis of the tube.

The radial profiles of the longitudinal and the transverse dimensionless fluctuation components $(\overline{V_\Theta'^2})^{1/2}$ and $(\overline{V_r'^2})^{1/2}$ (or in case of the pipe $(\overline{V_z'^2})^{1/2}$ and $(\overline{V_r'^2})^{1/2}$) differ either in their magnitude or in their course[9,13,14]. Apart from the almost monotonous course of both functions in case of the rotating cylinders and the courses exhibiting minima in the axis of the tube, they differ mainly in the form of the profiles of the longitudinal components. While in our apparatus the latter is almost con-

stant over the whole cross-section, in a tube the value of $(\overline{V_z'^2})^{1/2}$ between the wall and the axis doubles. The transverse component near the wall in the both cases steeply decreases which is more marked near the fixed cylinder than near the wall of the pipe. Both quantities compared differ also in the magnitude of the fluctuation component: in case of the rotating system the corresponding velocities are almost twice of these in the tube. This fact is well evidenced also in the radial profiles of the intensity of turbulence σ_θ and σ_r for the rotating system and σ_z and σ_r in a tube. In case of σ_θ and σ_z the difference in absolute magnitude is not so marked but in the pipe the intensity σ_z near the wall is twice as high as that in the axis of the tube. The course of the turbulent stress $\bar{\tau}'_{\theta r}$, or $\bar{\tau}'_{zr}$, differs also as a consequence of the mentioned facts: the monotonous course in the rotating system is widely different from that in a tube with two maxima.

From the comparison it follows that the field of turbulent characteristics in the space between the rotating inner cylinder with the blades and the outer solid cylinder at rest is a great deal more homogeneous than in a pipe and the intensity of turbulence in the former apparatus is much higher than in the latter. This will be particularly useful for processes involving dispersion of immiscible liquids[15]. Fot this reason as well as for the operating reasons (the size of the system and liquid hold-up) the proposed equipment may be regarded as well suited for the study of the transport phenomena in heterogeneous systems under steady supply of mechanical energy.

LIST OF SYMBOLS

A integration constant ($m^4\ s^{-2}$)
f friction factor
H height of apparatus (m)
K parameter
p static pressure ($kg\ m^{-1}\ s^{-1}$)
R radius of outer cylinder (m)
$Re_m \equiv [\bar{v}_{\theta max}(R - r_1)]/\nu$ Reynolds number
r radial coordinate (m)
r_1 radius of blade (m)
r_2 radius of the boundary between laminar sublayer and turbulent core (m)
$V_i \equiv \bar{v}_i/\bar{v}_{\theta max}$ dimensionless component of the mean velocity component
$(\overline{V_i'^2})^{1/2} \equiv (\overline{v_i'^2})^{1/2}/\bar{v}_{\theta max}$ dimensionless component of the fluetrating velocity
$\bar{v}$ local mean velocity ($m\ s^{-1}$)
$\bar{v}'$ local value of the fluctuation component of velocity ($m\ s^{-1}$)
$\bar{v}_{\theta max}$ mean peripheral velocity of the blades ($m\ s^{-1}$)
v^+ dimensionless mean velocity
$v^* = (\tau_w/\varrho_f)^{1/2}$ dynamic velocity ($m\ s^{-1}$)
z axial coordinate (m)
β universal constant
ε eddy viscosity ($m^2\ s^{-1}$)
Δp pressure drop ($kg\ m^{-1}\ s^{-1}$)
Δr_1 thickness of laminar sublayer (m)

Θ angular coordinate (deg)
ν kinematic viscosity ($m^2\ s^{-1}$)
σ_y standard deviation of y
σ_i intensity of turbulence of the i-th velocity component ($i = r, \Theta, z$)
$\varrho = r/R$ dimensionless radius
$\varrho^+ = \log [(1 + \varrho)/(1 - \varrho)]$ independent variable
ϱ_f density ($kg\ m^{-3}$)
$\bar{\tau}^t_{ij}$ time averaged component of turbulent stress tensor ($kgm^{-1}\ s^{-1}$)
τ_w viscous stress on the wall ($kg\ m^{-1}\ s^{-1}$)

Subscripts

i, j component in general direction
r radial component
z axial component
Θ tangential component

REFERENCES

1. Clay P. M.: Proc. Neder. Akad. Wet. *43*, 852, 979 (1940).
2. Gandhi R., Estrin J.: A.I.Ch.E.J. *17*, 349 (1971).
3. Ulbrecht J., Mitschka P.: *Chemické inženýrství ne-newtonských kapalin.* Academia, Prague 1965.
4. Ustimenko B. P., Zmejkov V. N., Buchman M. A.: *Turbulentnyje Těčenija*, p. 208. Izd. Nauka, Moscow 1969.
5. Schlichting G.: *Grenzschichttheorie* (in Russian). Izd. Nauka, Moscow 1969.
6. Mizushina T., Fujimoto K., Ito R., Hiraoka S., Tanaka M.: Chem. Eng. (Japan) *35*, 471 (1971).
7. Bird R. B., Stewart W. E., Lightfoot E. N.: *Transport Phenomena.* Wiley, New York 1965.
8. Knudsen J. G., Katz D. L.: *Fluid Dynamics and Heat Transfer.* McGraw-Hill, New York 1958.
9. Hinze J. O.: *Turbulence.* McGraw-Hill, New York 1959.
10. Pinkus O.: J. Appl. Mech. *19*, 425 (1952).
11. Soo S. L.: Chem. Eng. Sci. *5*, 57 (1956).
12. Mujumdar A. S., Huang B., Wolf D., Weber M. E., Douglas W. J. M.: Can. J. Chem. Eng. *48*, 475 (1970).
13. Mizushina T., Fukuda A., Ito R., Kataoka K., Nakashima Y.: Chem. Eng. (Japan) *35*, 1116 (1971).
14. Laufer J.: NACA Report 1174 (1954).
15. Steidl H.: This Journal *33*, 2191 (1968).

Translated by V. Staněk.